The atomic hydrogen flux to silicon growth flux ratio during microcrystalline silicon solar cell deposition

G. Dingemans, M. N. van den Donker, D. Hrunski, A. Gordijn, W. M. M. Kessels, and M. C. M. van de Sanden

The atomic hydrogen flux to silicon growth flux ratio during microcrystalline silicon solar cell deposition

G. Dingemans,[1] M. N. van den Donker,[1,a)] D. Hrunski,[2] A. Gordijn,[2] W. M. M. Kessels,[3]
and M. C. M. van de Sanden[3,b)]

[1]IEF5-Photovoltaik, Forschungszentrum Jülich GmbH, D-52425 Jülich, Germany and Department
of Applied Physics, Eindhoven University of Technology, P. O. Box 513, 5600 MB Eindhoven,
The Netherlands
[2]IEF5-Photovoltaik, Forschungszentrum Jülich GmbH, D-52425 Jülich, Germany
[3]Department of Applied Physics, Eindhoven University of Technology, P. O. Box 513, 5600 MB Eindhoven,
The Netherlands

The H flux to Si growth flux ratio is experimentally determined under state-of-the-art silicon thin-film deposition conditions by employing the recently introduced etch product detection technique. Under the technologically relevant high-pressure depletion conditions and for different process parameter settings such as pressure, SiH_4 concentration, rf power, and excitation frequency, it was demonstrated that the microcrystalline to amorphous silicon phase transition is uniquely and reactor independently determined by the flux ratio of H and Si growth species. © 2008 American Institute of Physics. [DOI: 10.1063/1.2987519]

The optimal phase composition of microcrystalline silicon (μc-Si:H) solar cell absorber layers is generally found in a narrow process window just before entering the amorphous growth regime.[1–3] The presence of atomic hydrogen is recognized as a key parameter influencing the crystallinity of the silicon films.[3–6] In the literature, it is often speculated that the hydrogen to Si growth precursor flux ratio should exceed a critical value for the nucleation of crystalline phase material to occur. Although the atomic hydrogen flux during deposition can in principle be determined by advanced techniques such as two-photon laser induced fluorescence or mass spectrometry,[7,8] the technologically relevant data available concerning the abundance of atomic hydrogen during μc-Si:H deposition remain largely based on correlations with indirect optical emission spectroscopy measurements and modeling work.[6,9–13]

Preferential insertion of atomic hydrogen in strained Si–Si bonds and subsequent silicon etching lead to a higher etch rate of amorphous silicon (a-Si:H) relative to crystalline Si.[14–16] In a recent Letter,[17] we demonstrated that this difference in etch rate can be exploited to determine *in situ* the phase composition of silicon films in the μc-Si:H growth regime. In this letter we introduce a quantification of the etch product density in terms of the absolute atomic hydrogen flux. We will show that within the studied parameter range the H flux to Si growth flux ratio uniquely determines the phase transition of μc-Si:H to a-Si:H (denoted by μc-Si $\rightarrow a$-Si). These data experimentally confirm the existence of a critical H flux to Si growth flux ratio.

A parallel plate plasma reactor (13.56 MHz, reactor A) with a substrate area of 10×10 cm^2 was used for most experiments.[2,17,18] High pressure depletion process settings included a power range (P_{rf}) of 60–120 W, a pressure (p_{dep}) range of 5–15 Torr, a substrate temperature of 200 °C, and a

H_2 flow (f_{H2}) of 360 SCCM (SCCM denotes cubic centimeter per minute at STP). For each fixed setting of p_{dep} and P_{rf}, the SiH_4 flow (f_{SiH4}) was varied between 0 and 10 SCCM to deposit films ranging from highly crystalline to purely amorphous silicon. Two other reactors were used for cross checking the experiments. In reactor B very-high-frequency excitation (95 MHz) was employed and process settings included an electrode gap of 5–10 mm, P_{dep} varying between 1.5 and 7.5 Torr, and showerhead or cross flow gas injection. Reactor C was a large area reactor with 30×30 cm^2 substrate area operated using deposition parameters similar to those for reactor A.[19]

An optical emission spectrometer allowed the collection of the plasma emission along the line of sight through a view port at the side of the reactors. Following the procedure described in Ref. 17, the phase composition of the as-deposited film (~ 150 nm thick) was probed by detecting the SiH* emission at 414.3 nm during a short H_2 plasma step. Deposition rates r_d were determined from thickness measurements by a step profiler. From r_d, the Si growth flux can be determined by multiplying it by the density of the deposited Si films ($\rho_{Si} \sim 5 \times 10^{22}$ cm^{-3}). Complete *p-i-n* solar cells were prepared by using ZnO coated glass substrates and 1×1 cm^2 back contacts of evaporated Ag. Solar cell performance was measured under 1000 W/m^2 AM 1.5 illumination at a temperature of 25 °C.

To determine the H flux during the H_2 plasma step, the baseline corrected SiH* emission intensity (I_{SiH^*}, in arbitrary units) was converted to an equivalent flow of SiH_4 etch products ($\Phi_{SiH4,etch}$) (in SCCM) in the procedure described below. Figure 1 shows I_{SiH^*} as a function of f_{SiH4} for two process conditions in reactor A ($P_{rf}=80$ and 120 W). Note that the SiH* emission at $f_{SiH4}=0$ is that part of the emission that can be attributed to the dissociation of etch products. The good linearity between I_{SiH^*} and f_{SiH4} strongly suggests that the presence of small SiH_4 fractions can be treated as an impurity in the H_2 plasma. The amount of etch product generated and the result of exposing the Si thin films to a H flux,

a)Present address: Solland Solar BV, Bohr 10, 6422 RL Heerlen, The Netherlands.
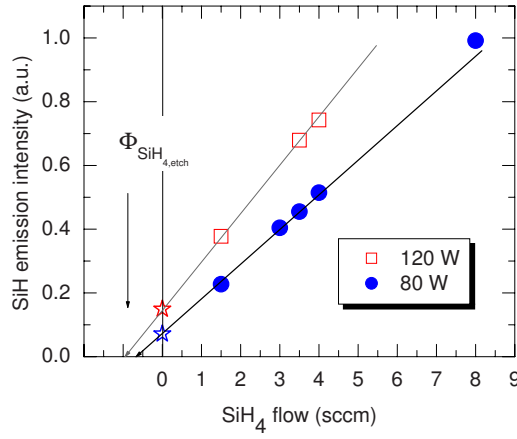b)Author to whom correspondence should be addressed. Electronic mail: m.c.m.v.d.sanden@tue.nl.

FIG. 1. (Color online) Baseline corrected SiH* emission intensity at 414.3 nm (I_{SiH*}) as a function of SiH$_4$ flow for 80 and 120 W rf power. Star symbols indicate I_{SiH*} during H$_2$ plasma probing. The x-interception (denoted $\Phi_{SiH4,etch}$) is the equivalent etching induced SiH$_4$ flow during H$_2$ plasma probing.

FIG. 3. (Color online) $\Phi_<$ (etch product flow with μc-Si:H film on substrate) for (a) different powers and (b) pressure conditions.

expressed in an equivalent SiH$_4$ flow $\Phi_{SiH4,etch}$, can be determined by extrapolating the linear fit to the x-intercept at $I_{SiH*}=0$. More information on the used linear dependence is given in Ref. 18. Note that this procedure should be repeated for every fixed plasma setting throughout a f_{SiH4} optimization series. Furthermore, note that a sound determination of $\Phi_{SiH4,etch}$ relies on the correct subtraction of the baseline when determining I_{SiH*}. We cross checked the baseline subtraction by measuring I_{SiH*} for $f_{SiH4}=0$ in a cleaned reactor with an uncoated substrate, in which indeed $I_{SiH*}=0$.

Figure 2 shows $\Phi_{SiH4,etch}$ corresponding to films deposited with various SiH$_4$ flows for the conditions $P_{rf}=80$ W and $P_{rf}=120$ W in reactor A. Three SiH$_4$ flow regions can be identified in Fig. 2(a): an initial plateau region, a steep increase, and a second (sloping) plateau region. From solar cell analysis, as well as Raman spectroscopy,[17] we deduced that
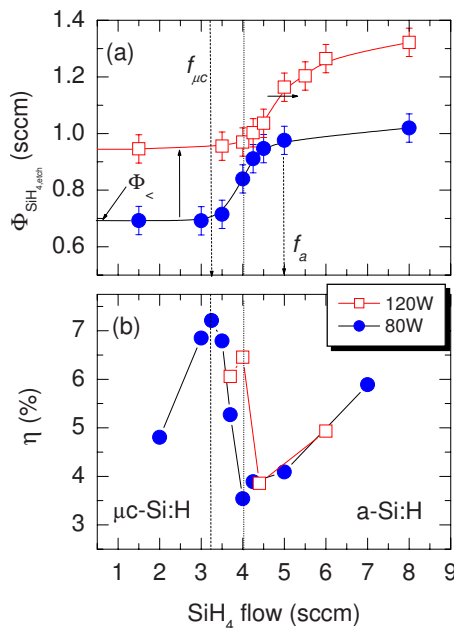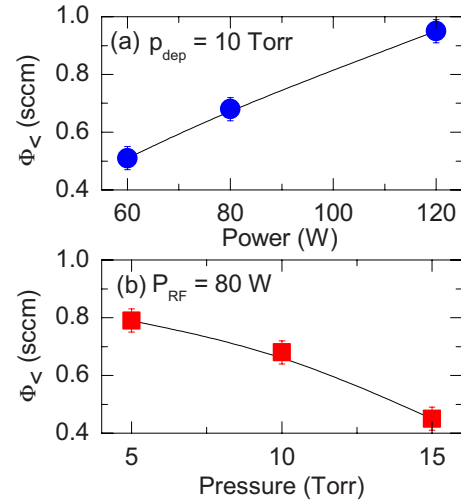

FIG. 2. (Color online) (a) SiH$_4$ etch product flow during H$_2$ plasma probing $\Phi_{SiH4,etch}$ as a function of the SiH$_4$ flow during deposition f_{SiH4} for $P_{rf}=80$ and 120 W. (b) Solar cell conversion efficiency η for the two corresponding series of solar cells.

the transition from the first plateau region to the steep increase coincides with the onset of the phase transition to mixed phase growth (at $f_{SiH4}=f_{\mu c}$).[17] We define the subsequent transition from the steep increase to the sloping plateau as the transition from mixed phase to amorphous silicon (at $f_{SiH4}=f_a$). In Fig. 2(b) we illustrate the correlation of etch product detection with the deposited material quality by showing the solar energy conversion efficiency η of solar cells deposited for both the 80 and 120 W series. Highest efficiencies were obtained for films deposited at the onset of the phase transition, i.e., at $f_{SiH4}=3.2$ SCCM for $P_{rf}=80$ W and $f_{SiH4}=4.0$ SCCM for $P_{rf}=120$ W.

Note that $\Phi_<$, defined as the etch product generation rate for etching of highly crystalline μc-Si:H films in the plateau region of Fig. 2(a), is observed to increase from 0.7 ± 0.05 to 0.95 ± 0.05 SCCM when increasing P_{rf} from 80 to 120 W. As has been mentioned above, the linearity between f_{SiH4} and I_{SiH*} (Fig. 1) and f_{SiH4} and the deposition rate[18] indicates that the influence of f_{SiH4} on the H flux can be neglected in a first approximation (for small SiH$_4$ concentrations, 0.2%–2%), and we can state that the H flux during deposition is equivalent to the H flux during H$_2$ plasma probing. We thus explain the higher $\Phi_<$ for higher P_{rf} in terms of a larger atomic hydrogen flux toward the film surface under these conditions. To investigate the dependence of the H flux on process parameters, we consider $\Phi_<$ in reactor A for various P_{rf} and P_{dep}. As can be seen in Figs. 3, $\Phi_<$ decreases with pressure and increases with power. These effects can be explained in terms of a lower electron temperature and smaller diffusion length for increasing pressure, and a rising electron density and dissociation rate of H$_2$ as a result of the increase in power.[20]

The H flux toward the film surface Γ_H (cm^{-2} s^{-1}), can now be expressed in terms of $\Phi_<$,

$$\Gamma_H = (\Phi_</A_{surface})/\gamma_{etch}, \qquad (1)$$

with γ_{etch} the etch yield of H atoms impinging on the film and $A_{surface}$ the total surface area exposed to the H flux (lower and upper electrode). $\Phi_<$ is given in particles per second (1 SCCM$=4.48\times10^{17}$ particles s^{-1}).

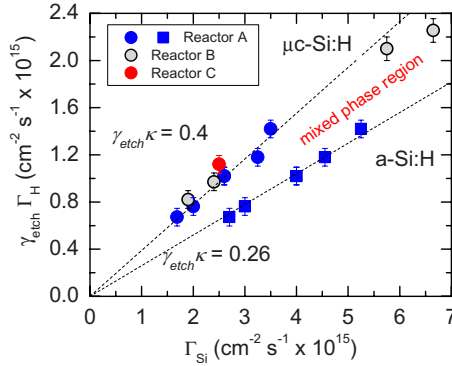To determine the *absolute value* of the H flux from Eq. (1), an appropriate value for the etch yield should be substi-

FIG. 4. (Color online) Phase diagram in the plane of the net silicon growth flux and a measure for the atomic hydrogen flux ($\gamma_{etch}\Gamma_H$). Circles indicate μc-Si:H growth conditions at the onset of the phase transition (at flow $f_{\mu c}$), whereas squares represent a-Si:H just after the complete transition (at flow f_a). Dotted lines along constant $\kappa\gamma_{etch}$ mark the transitions between the different phases.

tuted. Our results indicate that the etch yield is strongly dependent on the phase composition of the silicon film. In addition, factors such as substrate temperature, H-recombination probability, and ion bombardment should be taken into account for thorough analyses, as well as a possible difference in etch yield between the Si film on the upper electrode and on the lower electrode. For an order of magnitude estimate, however, an etch yield of 10^{-2} is assumed.[8,21] Therewith, from Fig. 3, H flux values between 6×10^{16} and 2×10^{17} cm^{-2} s^{-1} can be derived. Note that the order of magnitude of the H flux is in agreement with modeling results of high-pressure conditions of Lyka *et al.*[13]

To structure the discussion further, we introduce the dimensionless parameter κ, which is the ratio between the H flux Γ_H and the Si growth flux Γ_{Si},

$$\kappa = \frac{\Gamma_H}{\Gamma_{Si}} = \frac{(\Phi_</A_{surface})/\gamma_{etch}}{r_d\rho_{Si}}. \quad (2)$$

Next, we determined for the various power and pressure conditions of Fig. 3, the deposition rate for which the phase transition from μc-Si:H to the mixed phase ($a+\mu c$), and from $a+\mu c$ to a-Si:H occurred. From Fig. 3, we know $\Phi_<$ for the corresponding deposition regimes and thus using Eq. (1), the appropriate $\gamma_{etch}\Gamma_H$. By plotting $\gamma_{etch}\Gamma_H$ versus Γ_{Si}, we determined the slope $\kappa\gamma_{etch}$ for the transition data points in reactors A, B, and C. Figure 4 displays this main result of this letter and illustrates that the change in the phase composition of the material can be well described and understood in terms of only two parameters, namely, Γ_H and Γ_{Si}. A qualitative view on the data behind Fig. 4 is that in a f_{SiH4} optimization series (at constant P_{rf}, p_{dep}, excitation frequency or reactor geometry), the phase transition can be understood by variation in Γ_{Si} at constant Γ_H. When changing any of the parameters (P_{rf}, p_{dep}, excitation frequency, or reactor geometry), generally both Γ_H and Γ_{Si} change. However, the Γ_{Si} to Γ_H ratio $\kappa\gamma_{etch}$ at which the phase transition occurs, remains constant under the various reactor geometries and deposition conditions applied. This strongly suggests that the phase transition is uniquely determined by the H to Si growth flux ratio. These results might therefore indicate that under the used high-pressure high depletion deposition conditions the phase transition is a surface induced process, as $\kappa\gamma_{etch}$ re-

flects a ratio between the time constant related to the arrival rate of atomic H and the time constant related to the growth rate of 1 ML of silicon film.

Note that the absolute value for the H to Si growth flux ratio can be obtained by assuming again that γ_{etch} is in the order of 10^{-2}. We obtain $\kappa\approx40$ for the $\mu c\rightarrow a+\mu c$ phase transition. Conversely reasoned, to comply with the modeled estimates of Strahm *et al.*[11] ($\kappa\approx12$) and Klein *et al.*[3] ($\kappa\approx5$), slightly higher values for γ_{etch} between 0.03 and 0.05 seem more appropriate.

To summarize, the recently introduced technique of etch product detection was extended to determine the absolute H flux under μc-Si:H deposition conditions. From the H flux the ratio between the H and Si growth flux was determined in the phase transition regime for three different reactors and various plasma settings. From the results, we infer that the H to Si growth flux ratio at which the phase transition occurs is a constant, which strongly suggests that the phase transition is governed kinetically by the arrival rate of atomic hydrogen relative to the arrival rate of the growth precursors. The insights obtained provide an outlook to achieve high growth rates for silicon thin films in or close to the mixed phase region.

[1]O. Vetterl, F. Finger, R. Carius, P. Hapke, L. Houben, O. Kluth, A. Lambertz, A. Mück, B. Rech, and H. Wagner, Sol. Energy Mater. Sol. Cells **62**, 97 (2000).

[2]M. N. van den Donker, B. Rech, R. Schmitz, J. Klomfass, G. Dingemans, F. Finger, L. Houben, W. M. M. Kessels, and M. C. M. van de Sanden, J. Mater. Res. **22**, 1767 (2007).

[3]S. Klein, F. Finger, R. Carius, and M. Stutzmann, J. Appl. Phys. **98**, 024905 (2005).

[4]J. Kocka, T. Mates, H. Stuchlíková, J. Stuchlík, and A. Fejfar, Thin Solid Films **501**, 107 (2006).

[5]P. Roca i Cabarrocas and S. Hamma, Thin Solid Films **337**, 23 (1999).

[6]A. Matsuda, J. Non-Cryst. Solids **338-340**, 1 (2004).

[7]X. R. Duan, H. Lange, and A. Meyer-Plath, Plasma Sources Sci. Technol. **12**, 554 (2003).

[8]P. Kae-Nune, J. Perrin, J. Jolly, and J. Guillon, Surf. Sci. **360**, L495 (1996).

[9]L. Guo, M. Kondo, M. Fukawa, K. Saitoh, and A. Matsuda, Jpn. J. Appl. Phys., Part 2 **37**, L1116 (1998).

[10]E. Amanatides, D. Mataras, D. Rapakoulias, M. N. van den Donker, and B. Rech, Sol. Energy Mater. Sol. Cells **87**, 795 (2005).

[11]B. Strahm, A. A. Howling, L. Sansonnens, and Ch. Hollenstein, Plasma Sources Sci. Technol. **16**, 80 (2007).

[12]J. K. Rath, R. H. J. Franken, A. Gordijn, R. E. I. Schropp, and W. J. Goedheer, J. Non-Cryst. Solids **338-340**, 56 (2004).

[13]B. Lyka, E. Amanatides, and D. Mataras, J. Non-Cryst. Solids **352**, 1049 (2006).

[14]M. Otobe, M. Kimura, and S. Oda, Jpn. J. Appl. Phys., Part 1 **33**, 4442 (1994).

[15]I. Solomon, B. Drévillon, H. Shirai, and N. Layadi, J. Non-Cryst. Solids **164-166**, 989 (1993).

[16]M. Heintze, W. Westlake, and P. V. Santos, J. Non-Cryst. Solids **164-166**, 985 (1993).

[17]G. Dingemans, M. N. van den Donker, A. Gordijn, W. M. M. Kessels, and M. C. M. van de Sanden, Appl. Phys. Lett. **91**, 161902 (2007).

[18]M. N. van den Donker, B. Rech, W. M. M. Kessels, and M. C. M. van de Sanden, New J. Phys. **9**, 280 (2007).

[19]T. Kilper, M. N. van den Donker, R. Carius, B. Rech, G. Bräuer, and T. Repmann, Thin Solid Films **516**, 4633 (2008).

[20]E. Amanatides, S. Stamou, and D. E. Rapakoulias, J. Appl. Phys. **90**, 5786 (2001).

[21]J. Abrefah and D. R. Olander, Surf. Sci. **209**, 291 (1989).